Turbulent Kinetic Energy Budgets over Mountainous Terrain

THEODORE S. KARACOSTAS AND JOHN D. MARWITZ

Department of Atmospheric Science, University of Wyoming, Laramie 82071

(Manuscript received 2 October 1978, in final form 25 November 1979)

ABSTRACT

The objective of this study is to describe the characteristics of the airflow and turbulence structure over mountainous terrain. Turbulent characteristics of the airflow were measured using well-instrumented aircraft. The shear, buoyancy, transport of energy and eddy dissipation rate terms were obtained from direct measurements. The turbulent kinetic energy budgets were determined with respect to height and horizontal distance upwind and downwind of the mountain. The change of turbulence intensity was also demonstrated by comparing power spectra as a function of height, as well as a function of distance upwind and downwind of the mountain. The results show that all measurable terms were significant. The shear production and the eddy dissipation rate were the dominant terms. The buoyancy and vertical transport terms were smaller but still important. The imbalance term was estimated to be relatively small.

1. Introduction

Understanding the process of transport and turbulent diffusion of seeding material is a key component to the design and evaluation of cloud seeding experiments. The objective of this study is to describe the characteristics of the airflow and the turbulence structure over mountainous terrain. Turbulent kinetic energy (TKE) budgets will be presented from aircraft measurements. The TKE budget method is believed to be particularly instructive for this objective, since a detailed and complete knowledge of the source, maintenance and decay of the TKE can be accomplished. TKE budgets with respect to height at various locations, and with respect to the distance upwind and downwind of the mountain at several altitudes will be presented.

In Section 2 the aircraft instrumentation, statistical analysis, methodology and description of the Elk Mountain site are presented. The terms in the TKE budget model are discussed in Section 3. A particular case study of airflow and various TKE budgets are presented in Section 4. Section 5 contains a summary and conclusions.

2. Experimental procedures

The National Center for Atmospheric Research (NCAR) Queen Air 304D was flown upwind, over and downwind the orographic barrier of Elk Mountain (ELK), Wyoming. Turbulent characteristics of the air motion were obtained by measuring the longitudinal, lateral and vertical wind components along the aircraft track. A combination of precision Inertial Navigation Systems (INS), air sensing or gust probes and modern electronics have made it possible to record three-dimensional airflow and turbulence data from well-instrumented aircraft. An aircraft system is particularly powerful in being able to be flown over a variety of terrain features and in various situations.

a. Aircraft instrumentation

The sensors used by the Queen Air 304D were the air sensing probe for air measurements with respect to the airplane and the INS for determining the motion of the airplane with respect to the ground. The air sensing probe was located at the tip of a nose boom, and consisted of a pitot-static tube, two angle-of-attack vanes and a side-slip vane. The INS outputs, when combined with precise measurements of air motions relative to the aircraft (air sensing probe), are capable of resolving the mean and fluctuating components of the three-dimensional wind vector with respect to an earth-based coordinate system. Lenschow (1972) has estimated an accuracy of ± 1 m s^{-1} for mean velocities and ± 0.1 m s^{-1} for the fluctuating components.

The outputs of the instruments were first recorded digitally and later converted to computer-compatible magnetic tape. Wind vector components and temperature were digitized at 16 Hz, and later averaged to 8 Hz.

b. Methodology

The longitudinal and lateral wind components along the aircraft track, measured directly by the Queen Air, have been combined trigonometrically

0021-8952/80/020163-12$07.00

to compute the longitudinal (u') and lateral (v') wind components with respect to the mean wind direction. The fast Fourier transform (FFT) technique has been used for the analysis of the flight data. This method was adopted due to the double advantage of ease of interpretation and computational speed.

Each flight segment was partitioned into blocks of 512 data points (64 s). Means and trends were removed from each of the individual blocks, and only the fluctuation quantities were used in the TKE budget calculations. Therefore, the stochastic processes $u'(t)$, $v'(t)$, $w'(t)$ and $\theta'(t)$ have a zero mean, a digitization interval of $\Delta t = 0.125$ s, a Nyquist frequency of $f_n = 4$ Hz and a resolution of $R = 0.016$ Hz. Each block from the entire flight segment was dealt with separately, producing a family of power spectra which were averaged together, yielding averaged spectra for each of the three wind vector components and potential temperature.

c. Site description

Elk Mountain is an isolated peak at the north end of the Medicine Bow Mountains in southeastern Wyoming. This three-dimensional mountain peak rises to an elevation of ~3400 m MSL, above a relatively flat terrain of ~2100 m MSL. The mountain is characterized by a gradual upwind slope and a steep downwind slope. The eastern slope descends ~920 m over a distance of less than 4 km. A vertical west–east cross section of ELK is presented in Fig. 4.

3. Theory

a. Turbulent characteristics in the inertial subrange

A dimensional analysis predicts that within the inertial subrange the TKE per unit wavenumber, or spectral density, will vary according to the Kolmogorov-Obukhov ⅔ law for the structure function, and according to the Kolmogorov $-5/3$ law for the spectrum in wavenumber domain. This is expressed mathematically in the Kolmogorov equation

$$E(k) = \alpha\epsilon^{2/3}k^{-5/3}. \tag{1}$$

The transformation of Eq. (1) from wavenumber domain to frequency domain, in which the aircraft data are conveniently expressed, is given by

$$E(f) = \alpha(\mathrm{TAS})^{2/3}(2\pi)^{-2/3}\epsilon^{2/3}f^{-5/3}, \tag{2}$$

where TAS is the true air speed.

Lumley and Panofsky (1964) suggest that the universal constant α is valid only for the one-dimensional spectral law of the longitudinal (with respect to the mean wind direction) velocity component. For lateral and vertical velocity component, the proper constant would be $(4/3)\alpha$. Recent determinations of the universal constant suggest that α is between 0.45 and 0.50, with accuracies of 20 and 14%, respectively (Vinnichenko *et al.*, 1973). In this particular study, α will be assumed to be 0.50 for the spectral law of the longitudinal velocity component, which is consistent with the value used by Caughey and Wyngaard (1979). For the spectral laws of the lateral and vertical velocity components α will be assumed to be 0.67.

b. The turbulent kinetic energy budget model

In high Reynolds number atmospheric turbulence, the budget of TKE per unit mass can be expressed as

$$\frac{\partial}{\partial t}\tfrac{1}{2}(\overline{u_i'u_i'}) + \overline{u_i'u_j'}V_{i,j} + V_j\overline{u_i'u_{i,j}'} + \overline{u_i'u_{i,j}'u_i'} - \overline{u_i'\overline{u_{i,j}'u_j'}} = -\frac{1}{\rho}\overline{u_i'p_{,i}'} + \overline{\nu u_i'u_{i,jj}'} + \frac{g}{\bar{\Theta}}\overline{u_i'\theta'}\delta_{3i}. \tag{3}$$

Eq. (3) has been derived from the governing equations (equation of motion and the incompressible form of the continuity equation) for the fluctuating quantities (Lumley and Panofsky, 1964), using Cartesian tensor notation and the Einstein summation convention. Here V_i and u_i' are the mean and fluctuating parts of wind velocity in the x_i direction, respectively. The overbar and capital letters denote time average. The above equation simplifies considerably using the Boussinesq approximation and the assumption of horizontal homogeneity, where mean quantities vary only in the vertical and have only a streamwise component. Thus, the TKE budget equation in the boundary layer, converted to the Cartesian coordinate system, can be written as

$$\frac{\partial\bar{e}}{\partial t} = \frac{\boldsymbol{\tau}}{\rho}\cdot\frac{\partial\mathbf{V}}{\partial z} - \frac{\partial}{\partial z}\left[\frac{1}{\rho}(\overline{w'p'}) + \overline{w'e}\right] + \frac{g}{\bar{\Theta}}\overline{w'\theta'} - \epsilon, \tag{4}$$

where $\boldsymbol{\tau}$ is the mean shear stress obtained from

$$\frac{\boldsymbol{\tau}}{\rho} = -(\overline{u'w'})\mathbf{i} + (\overline{v'w'})\mathbf{j}. \tag{5}$$

In Eq. (4), $\partial\bar{e}/\partial t$ represents the local rate of change of the TKE. Except during transitional periods in the turbulence regime, this term is expected to be generally small compared with the other terms. Lenschow (1974) found this term to be typically two orders of magnitude smaller than the other terms in the boundary layer. A similar result was found in the Minnesota experiment (Caughey and

Wyngaard, 1979). This does not mean necessarily that it is negligible over the mountainous terrain case considered here. However, we will neglect it in this study.

The first term on the right-hand side in Eq. (4), $\tau/\rho \cdot \partial \mathbf{V}/\partial z$, represents the rate of TKE supply to the budget through shearing forces of the mean wind by the Reynolds stresses.

The pressure transport term, $\rho^{-1}\partial(\overline{w'p'})/\partial z$, represents the transfer of energy from one point in space to another point due to fluctuating pressure. This term remains the least well-understood term in the TKE budget equation. The pressure transport term cannot be determined easily from aircraft measurements because of the difficulty in measuring small fluctuating static pressure. In spite of recent evidence about the significance of this term, it will be neglected in this study.

The third term in Eq. (4), $\partial(\overline{w'e'})/\partial z$, is the vertical divergence of transport of turbulent kinetic energy. This term was obtained by calculating $\overline{w'e}$ at each flight level and dividing the difference between two successive levels by the difference in height. Since the calculation of this term involves a vertical derivative of third-order moment, large scatter is expected.

The fourth term $(g/\bar{\Theta})\overline{w'\theta'}$, represents the rate of work against the buoyancy forces. This term could be either a source or a sink, depending on the sign of the vertical heat flux.

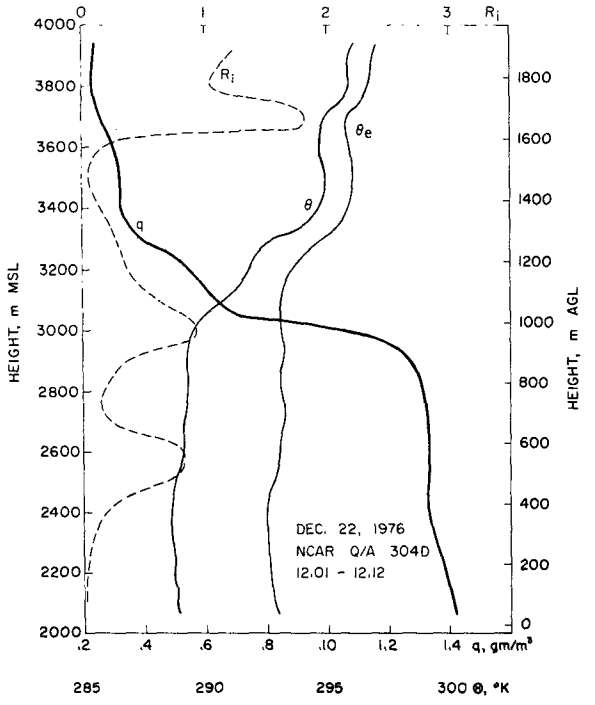

FIG. 1. Aircraft sounding for 22 December 1976. Potential temperature (θ), equivalent potential temperature (θ_e), specific humidity (q) and gradient Richardson number (Ri) are shown.

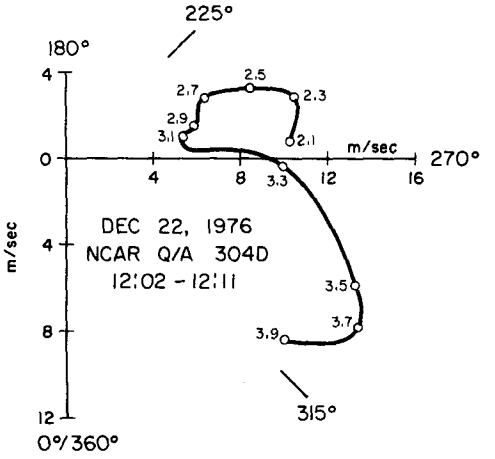

FIG. 2. Hodograph of winds from 2.1 to 3.9 km. The winds (m s^{-1}) were measured upwind of ELK.

The last term ϵ is the rate of conversion of TKE into internal energy, the eddy dissipation rate. The ϵ term was calculated from the longitudinal (with respect to the mean wind direction) spectrum, by fitting the $-5/3$ power law, according to Kolmogorov's theory for the inertial subrange [Eq. (2)].

It seems intuitively obvious that mountain-induced turbulence is inhomogeneous. Thus, when comput-

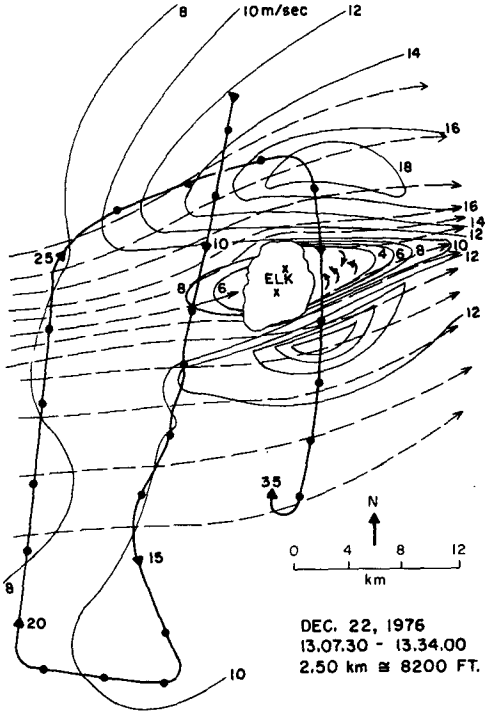

FIG. 3. Airflow analysis over ELK on 22 December 1976 at 2.5 km MSL. The heavy solid line shows the flight track, the thin solid lines present the isotachs (m s^{-1}), while the dashed lines indicate the streamlines. Closed circles along the flight track represent 1 min intervals and arrows represent 5 min intervals.

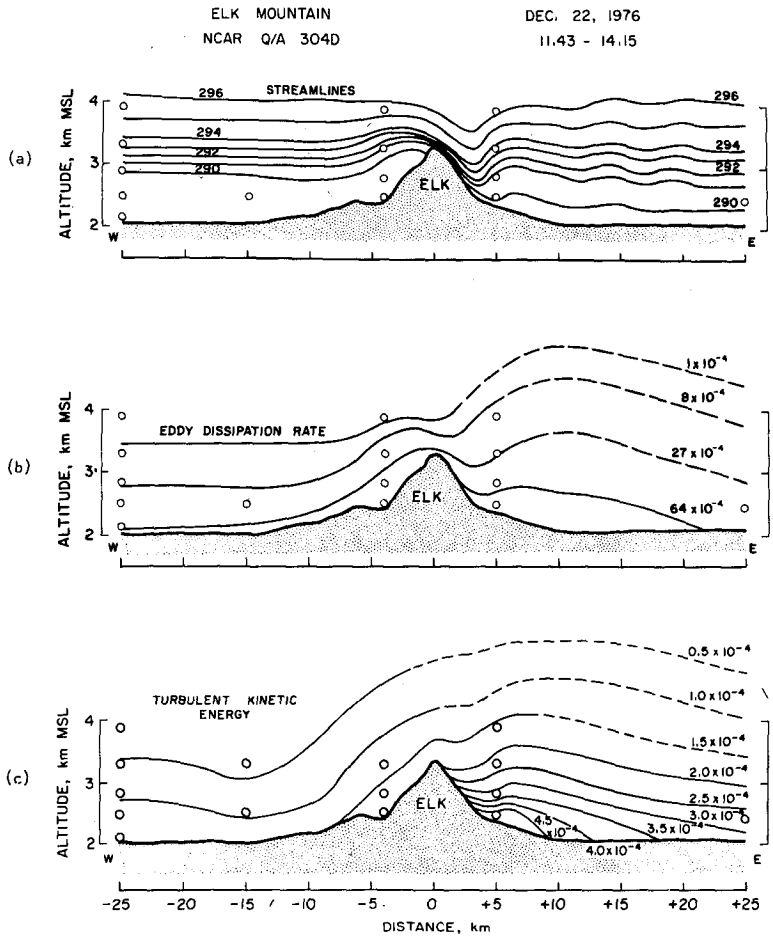

FIG. 4. Vertical west–east cross section over ELK of a) streamline analysis using potential temperature, b) eddy dissipation rate ($m^2 s^{-3}$) analysis and c) turbulent kinetic energy ($m^2 s^{-2}$) analysis.

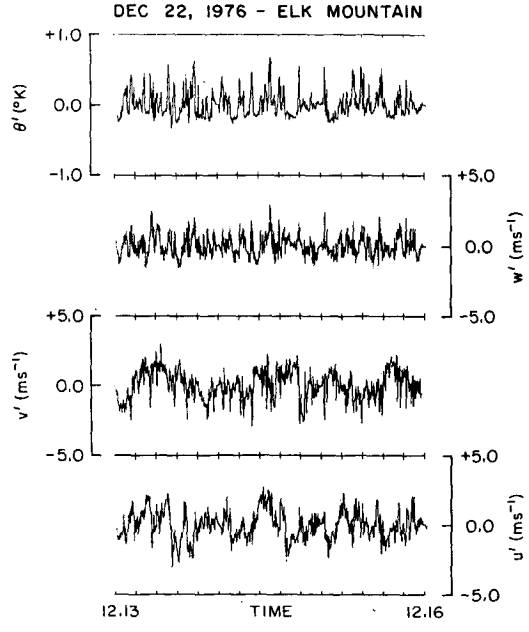

FIG. 5. Time series of longitudinal (u'), lateral (v') and vertical (w') wind components, with respect to the mean wind direction, as well as of potential temperature (θ'), for 22 December 1976. They correspond to flight segments at 2.15 km MSL, observed ~25 km upwind of ELK.

ing the TKE budget in mountainous terrain, inhomogeneity effects were considered. However, due to the very carefully chosen flight segments used for the spectral analysis, the Runs test (Mendenhall and Schaeffer, 1973) did not reject the hypothesis of homogeneity and stationarity at the level of significance of 0.05, for ~95% of the flight segments, implying general homogeneity along the flight segments. Observational errors, statistical sampling errors, errors involved in assuming homogeneity and stationarity, and errors in neglecting the pressure transport and horizontal advection terms are combined in an imbalance or residual term I.

Incorporating these assumptions, we can rewrite Eq. (5) as

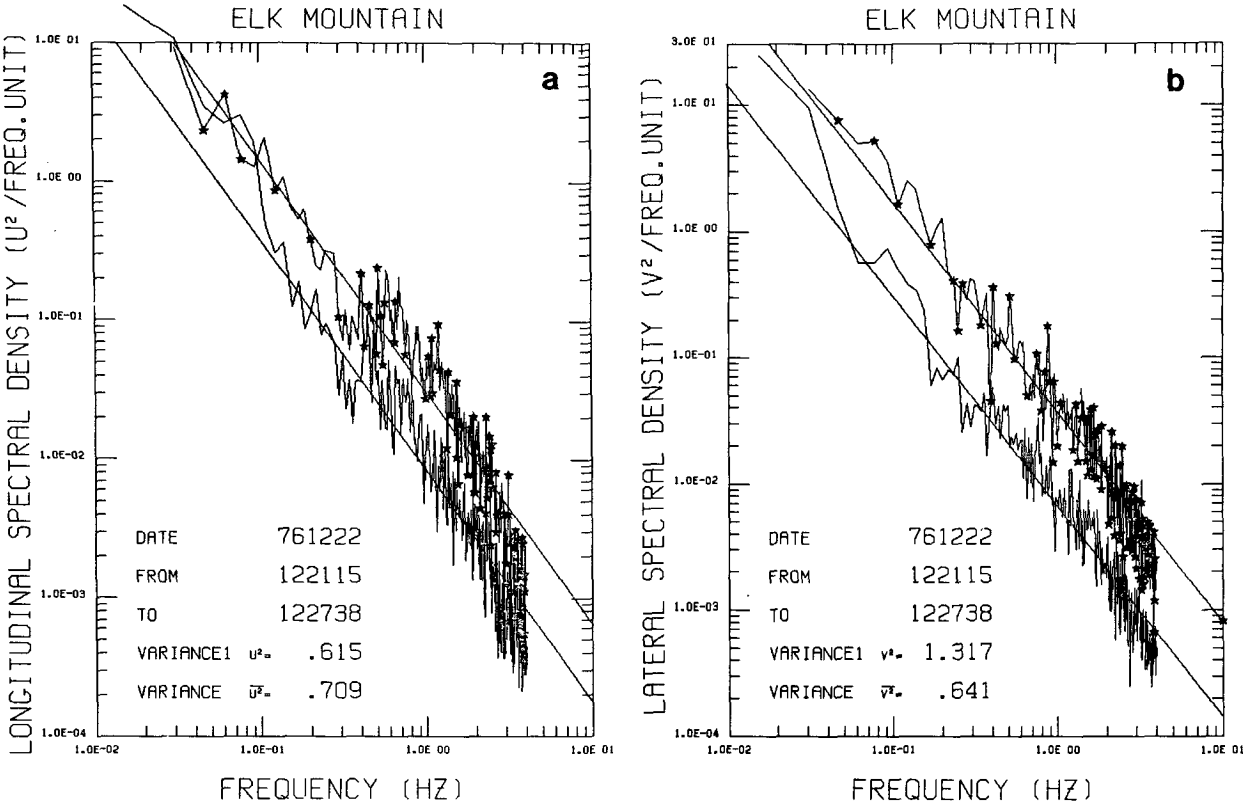

FIG. 6. Power spectra of a) longitudinal (u'), b) lateral (v'), and c) vertical (w') with respect to the mean wind components. The straight lines represent the $-5/3$ power law. The asterisks and VARIANCE 1 correspond to the lower altitude.

$$\frac{\tau}{\rho} \cdot \frac{\partial \mathbf{V}}{\partial z} - \frac{\partial}{\partial z}(\overline{w'e}) + \frac{g}{\bar{\Theta}} \overline{w'\theta'} - \epsilon + I = 0, \quad (6)$$

which is the form of the TKE budget equation used in this study.

c. *Previous work*

All measurements of the TKE budget to date have been done over homogeneous terrain.

Myrup (1969), Zubkovskiy and Koprov (1970), Lenschow (1970, 1973), Pennell and LeMone (1974) and Eaton and Dirks (1977) used instrumented aircraft in the boundary layer for direct measurements of most of the terms in the budget. In the first two studies, the vertical transport of TKE and pressure fluctuation terms were not measured. Lenschow (1970, 1973), Pennell and LeMone (1974) and Eaton and Dirks (1977) calculated the vertical transport of TKE. The eddy dissipation rate was estimated from the spectral density in the inertial subrange.

Wyngaard and Coté (1971) made a detailed study of the TKE budget in the surface layer. They used direct measurements of turbulent energy production

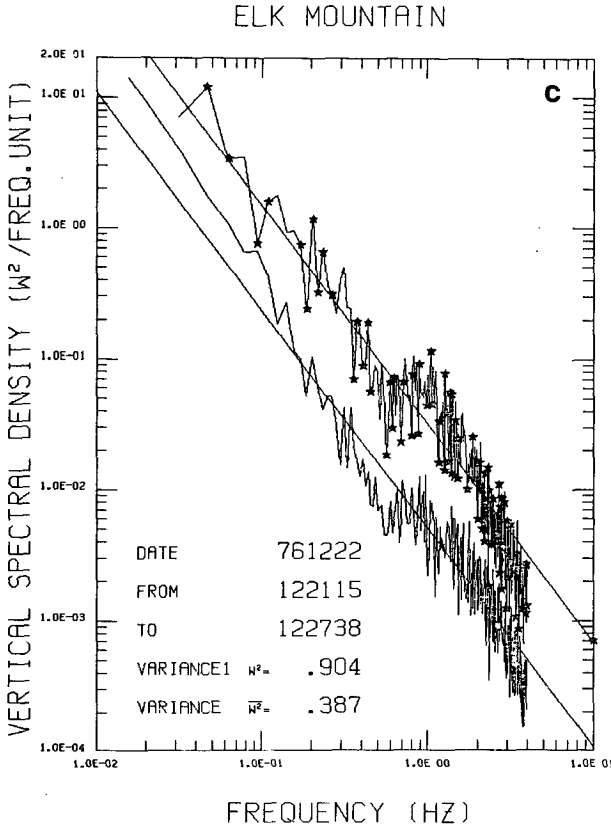

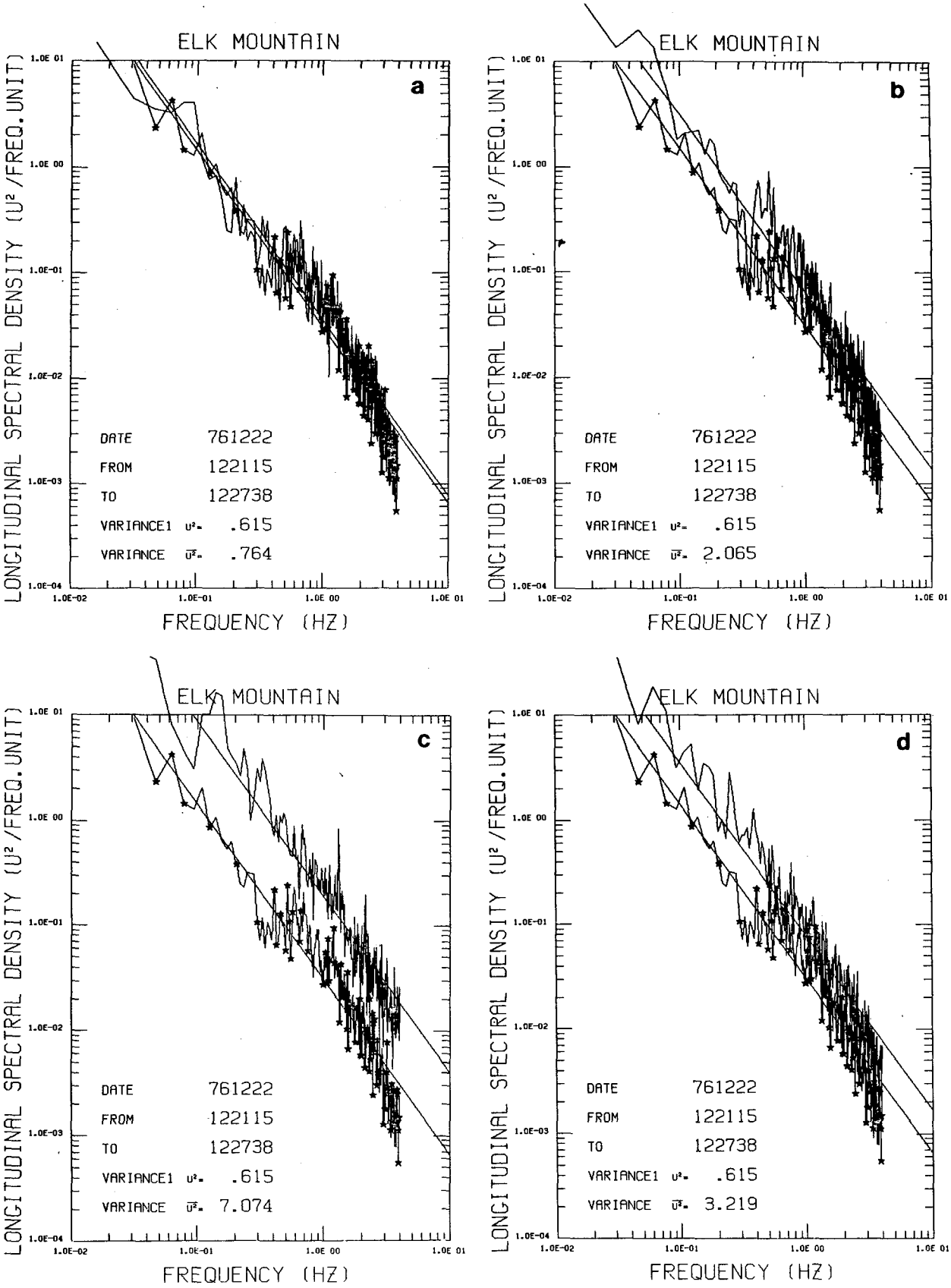

by both shear and buoyancy, the vertical transport of turbulence and the eddy dissipation rate. Their residual term was due to pressure fluctuations (which were not measured) and to experimental difficulties such as horizontal inhomogeneity. Recent TKE budget studies in the boundary layer confirmed the existence of the imbalance term and relate this to the pressure transport term (Champagne *et al.*, 1977; Caughey and Wyngaard, 1979).

In summary, the shear term, buoyant term and transport of turbulent energy term can be calculated from actual turbulent flux measurements of momentum and heat and the aircraft sounding. The eddy dissipation rate term can be calculated by fitting the $-5/3$ power law to the power spectra.

4. 22 December 1976—Case study

The 22 December 1976 case study was selected for presentation because the flight routines were complete and the airflow was thought to be representative for a large number of airflow cases over ELK.

a. Synoptic conditions and aircraft flight

The 500 mb analysis for this date shows a relatively large-amplitude long-wave trough positioned over the High Plains, giving north-westerly airflow over the experimental area. In association with an upper air ridge along the west coast, a surface high-pressure system was located over the Oregon–Idaho area with associated subsidence in Wyoming.

The NCAR Queen Air was flown upwind and downwind of ELK nearly 100 min collecting raw turbulence data. Several passes were made perpendicular to the wind at various upwind and downwind distances of the peak, at five different altitudes. (The crosswind aircraft passes were necessary for safety purposes.) The aircraft was flown in constant heading and at approximate mean TAS of 75 m s^{-1}. The vertical profile of equivalent potential temperature (θ_e), potential temperature (θ), specific humidity (q) and gradient Richardson number (Ri), were made while descending at constant heading ~25 km upwind of ELK (Fig. 1). The vertical θ_e profile indicates near-neutral or slightly stable thermodynamic stability below 3.0 km MSL topped by a 4 K stable layer from 3.0 to 3.4 km MSL. Above 3.4 km MSL the thermal structure indicated neutral thermodynamic stability. The Ri profile indicated possible dynamic instability between 2.7 and 2.9 km MSL and between 3.2 and 3.6 km MSL. The wind hodograph from the aircraft sounding is presented in Fig. 2, demonstrating the strong wind shear between 3.1 and 3.7 km MSL, where the winds veer with height.

b. Airflow

Although complicated by the three-dimensional nature of the flow, the Elk Mountain airflow features correspond to those observed in studies such as gravity waves and hydraulic jumps. Fig. 3 shows the airflow around ELK at 2.5 km MSL. The heavy solid line represents the flight track, along which data were obtained to produce the airflow analysis.

The streamlines diverge on the windward side of the mountain and converge behind it, causing the air to flow up the lee slope. A flow separation occurred due to a contribution of factors including the adverse pressure gradient, the friction and the shape of the mountain. A reverse eddy type flow occupied the space between the separated streamlines and the mountain. The separated area was characterized by generally high mixing rates, lower wind speed and regions of systematic reverse flow. This reversal flow was accompanied by the formation of a large semi-permanent eddy. From Fig. 3, it can be seen that the wind speed increased along either side of the mountain. Due to the flow separation, two high speed jets of 18 m s^{-1} were present on each side of the mountain. More extensive downwind data show that the flow separation does not exist further downwind (Karacostas, 1978).

Fig. 4a presents a west–east vertical cross section of ELK with a streamline analysis from aircraft measured potential temperature. The packing of the isentropes between 290 and 294 K indicates the stable layer which separates the stable and well-mixed layer. Circles represent the 15 aircraft passes at five different altitudes which were used in the TKE budget calculations.

c. Statistical analysis

The maximum wavelengths observed in the horizontal and vertical velocity spectra were estimated to be 2.5 and 0.9 km, respectively. These wavelengths correspond to the length scale of the larger eddies that appear to dominate the circulation in the boundary layer. This result is based on the following spectral analysis procedure. Based on data collected over ELK, the non-monotonic function, $fE(f)$ where f is frequency, was calculated and plotted versus $\ln f$, for the frequency range of 0.0039 to 4 Hz (equivalent wavelength range 20 km to 20 m). This energy spectrum, in which the area under the spectral curve indicates the contribution of specific frequency bands to the total variance, peaked at maximum wavelengths of 2.5 and 0.9 km for horizontal and vertical velocity spectra, respectively. These results seem to be consistent with LeMone's (1973)

FIG. 7. Power spectra for u' at a) −15 km, b) −4 km, c) +5 km, and d) +25 km from ELK, in well-mixed layer. The asterisks and VARIANCE 1 correspond to 25 km upwind of ELK.

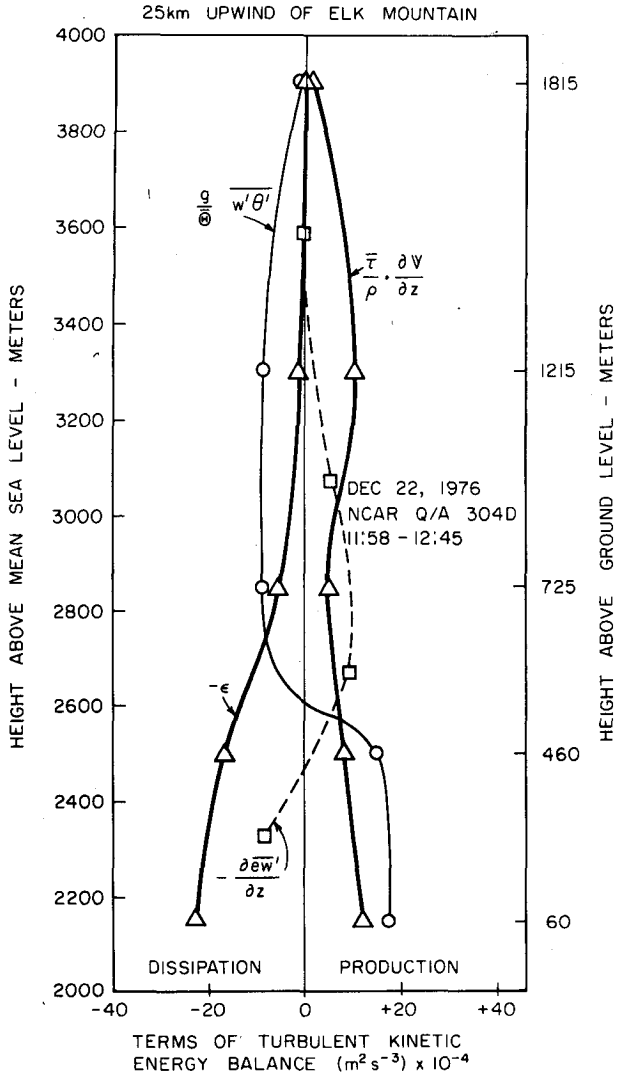

FIG. 8. Vertical profile of TKE budget at ~25 km upwind of ELK. Each plotted point represents an average for several different blocks over the entire flight leg.

indications that the maximum wavelength of horizontal roll vortices is roughly three times the size of the boundary layer thickness, which is <1 km (Fig. 1). Further, recent studies by Kaimal *et al.* (1976) have shown that the maximum wavelength for the horizontal eddies is approximately 1.5 times the size of the boundary layer thickness. Therefore, we have used the "blocking" technique with blocks of 64 s (~5 km) because this gives a statistically sufficient sample for 2.5 km wavelengths. The use of the blocking technique has some statistical advantages: 1) the time series within the individual blocks are homogeneous and stationary, and 2) the spectral estimates obtained from averaging the spectral lines from the individual blocks are statistically more stable because of the increased degrees of freedom.

d. Turbulence power spectra

A time series sample of u', v', w' and θ' is presented in Fig. 5. The data were observed ~25 km upwind of ELK and at an altitude of 2.15 km MSL (~60 m AGL). Fig. 6 presents some power spectra of u', v' and w'. These data were also observed ~25 km upwind of ELK. The flight passes are indicated by circles in Fig. 4, and correspond to altitudes at 2.5 and 3.3 km MSL. Spectral lines indicated by asterisks and the value of VARIANCE 1 correspond to the lower altitude flight segment. The straight lines represent the $-5/3$ power law fitted for frequencies higher than 0.06 Hz. Fig. 6 demonstrates the variation of spectral densities and hence turbulence intensities of the three wind vector components as a function of height.

The variation of spectral densities, variances and thus turbulence intensities for the longitudinal wind component is presented in Fig. 7 for various horizontal distances from ELK. The power spectrum corresponding to the flight segment at ~25 km upwind of ELK is plotted on each diagram for comparison. This flight segment was compared with four other flight segments, all of them being in the well-mixed layer. As expected, the spectral energy, variance and turbulent intensity increased as one approaches the mountain. Their maxima occurred downwind and very close to the mountain. The values gradually decreased as one moved further away from the mountain. Similar but smaller variations were noticed by comparing power spectra in the stable layer, upwind and downwind of ELK. Little variation was present among power spectra above the stable layer.

e. The turbulent kinetic energy budget

The well-executed flight mission and the high quality of data made it possible to derive a detailed quantitative and qualitative presentation of TKE budgets, with respect to height at various locations and with respect to horizontal distance upwind and downwind at various altitudes.

The magnitudes of the four terms of the TKE budget model [Eq. (6)] have been estimated from the calculated power spectra with blocks of 512 data points, time series and the aircraft sounding and hodograph. Variances and Reynolds stresses (covariances) were calculated in two different ways; first, based on their definition, by averaging the product of time series, and second based on their property, by integrating the area under the spectral or cospectral density lines. The vertical gradient of the wind velocity vector was calculated from the wind hodograph.

The eddy dissipation rate term has been calculated in the wavelength range of 1200–20 m, from the spectra with blocks of 512 data points. In addition ϵ

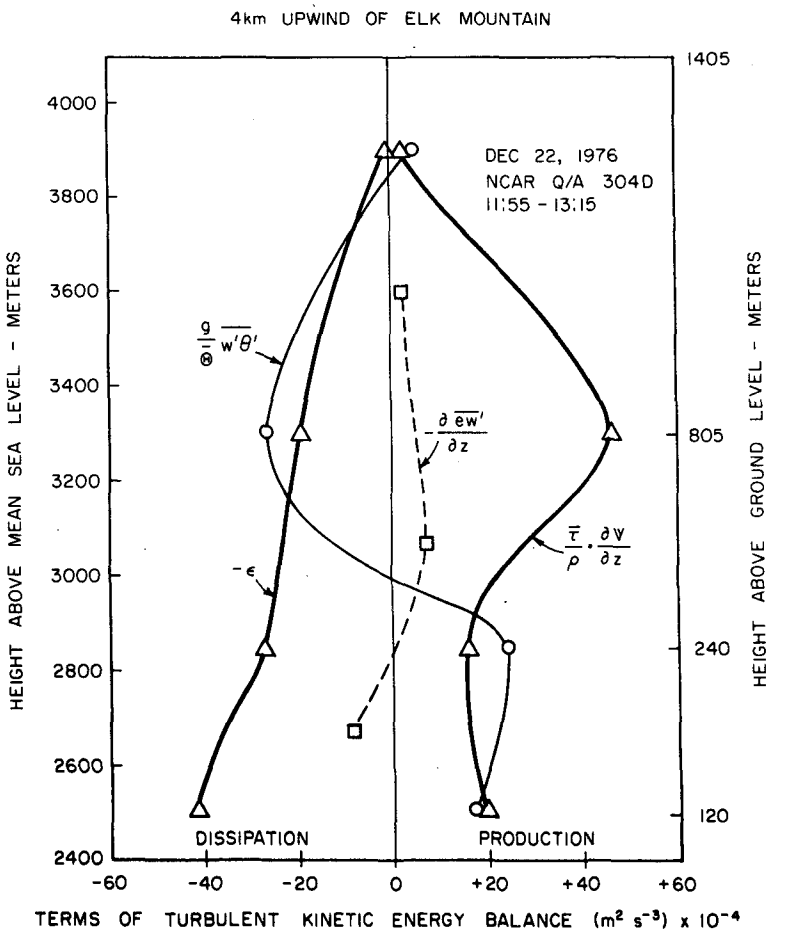

FIG. 9. As in Fig. 8 except at ~4 km upwind of ELK.

values have been calculated in the wavelength ranges of 800–20 m and 400–20 m, from spectra with blocks of 256 and 128 data points, respectively. The means and standard deviations of the $\epsilon^{1/3}$ values were computed for each leg using 256 and 128 data point blocks. The Student's t test indicated that the means computed for each leg from the two different blocking lengths were not significantly different. This suggests that the turbulence was stationary within each block. Examination of the values of the standard deviations of $\epsilon^{1/3}$ with respect to the mean $\epsilon^{1/3}$ shown in Fig. 4b is useful. The standard deviation of $\epsilon^{1/3}$ varied from ~0.3 upwind of ELK to ~0.7 over the upwind slope to ~1.5 in the immediate lee of ELK to ~0.6 far downwind of ELK. Since the mean exceeded the standard deviation by a factor of 3 at all locations, this suggests that the turbulence was stationary.

TKE budgets with respect to height are presented in Figs. 8 and 9, at distances of 25 and 4 km upwind of ELK, while Fig. 10 shows the TKE budget with respect to height at 5 km downwind of ELK. It is apparent that these budgets are dominated by two terms: the shear production term and the eddy dissipation rate term.

The shear production term is considered to be one of the two most important terms in the TKE budgets, because of the significant contribution to the production of energy in the well-mixed layer and in the layer with stable thermodynamic stability. In Fig. 8 the shear term is almost constant with height, which is quite reasonable due to the large distance from the mountain and also the light turbulence condition. The high shear-produced energy shown in Fig. 9 at the altitude of ~3.3 km MSL seems to be consistent with the observed turbulence conditions and wind hodograph. Due to the stable layer at that altitude, the shear-produced energy would have to be transported downward to the well-mixed layer, either by the vertical transport term or the pressure transport term. From Figs. 8–10 it may be seen that the shear-produced energy becomes more pronounced, closer and downwind of the mountain. The variation of the shear production term is clearly demonstrated in Fig. 11, which presents the TKE budget at 2.5 km MSL as a function of horizontal

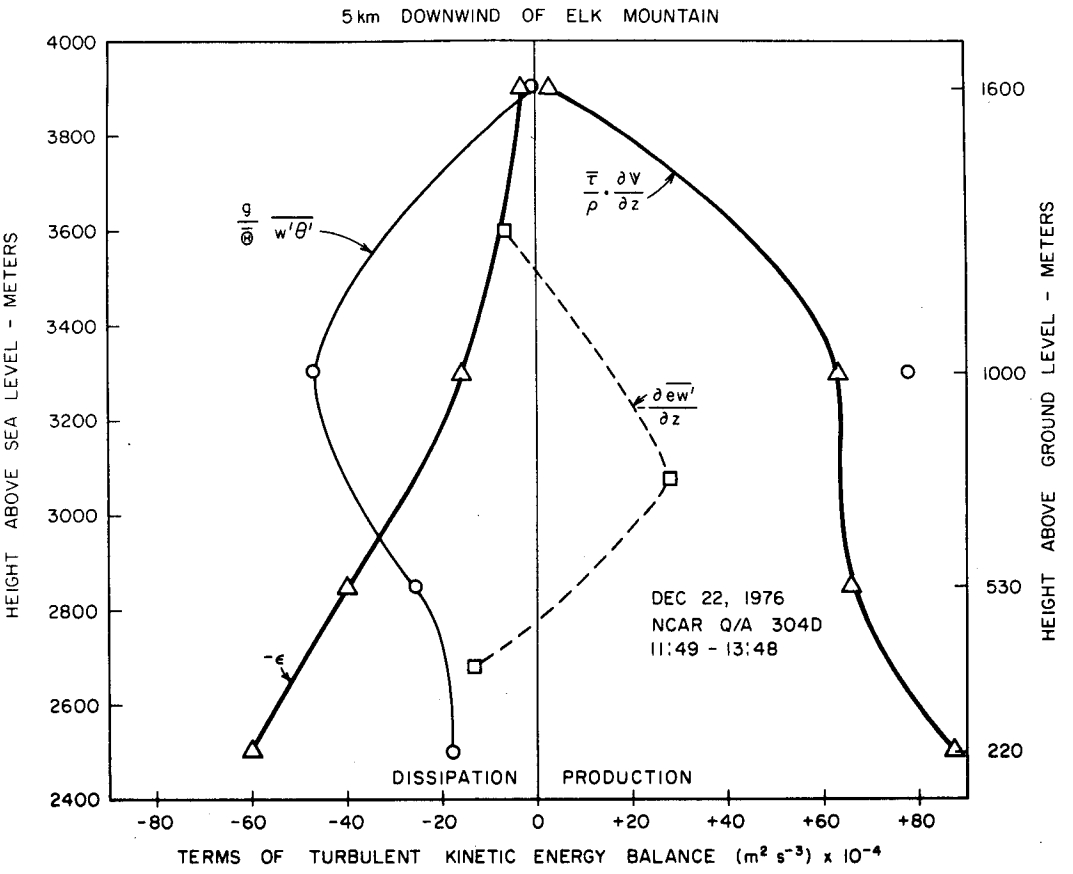

FIG. 10. Vertical profile of TKE budget at ~5 km downwind of ELK. Each plotted point represents an average for several different blocks over the entire flight leg.

distance upwind and downwind of ELK. In Fig. 11, the vertical transport of energy term has been omitted due to the lack of data at this low level.

The other important term in the TKE budgets is the eddy dissipation rate term. In the upwind area (Figs. 8 and 9), ϵ is seen to gradually decrease with increasing stability. By comparison, in the downwind area (Fig. 10), ϵ decreases rapidly with height in the well-mixed and stable layers. Above the stable layer, ϵ appears to approach a constant value with height. Fig. 11 shows that ϵ decreases rapidly with distance downwind of the mountain, tending to approach values similar to the ones present in the upwind area. The same phenomenon can also be observed for the shear production term. Fig. 4b represents a vertical cross section of the eddy dissipation rate analysis over ELK. The different turbulence structure upwind and downwind of the mountain is apparent. These both demonstrate the importance of topography to turbulence structure.

The buoyancy term plays a significant role in the TKE budgets. Upwind of the mountain and in the well-mixed layer it appears as a significant production term. It combines with the shear production term to balance the energy losses due to the eddy dissipation rate term. In stable and neutral thermodynamic stability conditions, the buoyancy term becomes negative and decreases gradually with height to an almost negligible value at 3.9 km MSL. In the downwind area, the buoyancy term appears as a dissipation term at all altitudes.

A rather interesting phenomenon was observed downwind of ELK. A buoyant eddy of less than 1 km in size was detected by the aircraft resulting in a very high positive vertical heat flux destroying the balance among the other terms of the TKE budget. Upon removing that large buoyant eddy from the flight segment, a negative vertical heat flux resulted and a balance in the TKE budget was observed. This phenomenon is presented in Fig. 10 at 3.3 km MSL where the circle at the far right side of the figure is the buoyancy term when the buoyant eddy is retained. The existence of that large buoyant eddy is not well understood. However, two alternatives are possible. Either it is a persistent eddy, due to hydraulic jumps which frequently occur downwind of ELK and an unbalanced situation is actually present or the buoyant eddy is an intermittent phenomenon and therefore the balanced situation is the normal case downwind of ELK.

The buoyancy suppression seems to be related to the rapid decrease of the eddy dissipation rate with height. This is because thermals generated in the well-mixed layer are dissipated in the stable layer.

Finally, the vertical transport of the energy term, although the least important term, plays a significant role in the TKE budgets, by transporting energy by turbulence out of the lower portion of the well-mixed layer into the higher levels. As neutral conditions are approached the vertical transport of the energy term tended to become negligible, denoting a trend toward balance among the shear production term, the eddy dissipation rate term and the buoyancy term.

5. Summary and conclusions

The variances, Reynolds stresses and power spectra presented in this study are valuable for diagnosing the structure and characteristics of the atmospheric turbulence over mountainous terrain. Although the horizontal (longitudinal and lateral) estimated spectral densities seemed to have more energy than the vertical, all of them fall off gradually with increasing frequency. It has been shown that the turbulence intensity and the magnitude of the spectral density lines are strongly related to the wind shear, stability and roughness of the terrain.

From the TKE budgets it is concluded that all the measurable terms are significant. It was found that the budgets were dominated by the shear production and the eddy dissipation rate terms. The other two terms, the buoyancy and the vertical transport terms, were smaller but still important.

In the well-mixed layer of the upwind area, the turbulent kinetic energy generated through buoyancy forces is transported out of the layer, and the eddy dissipation rate seems to balance the shear production and the buoyancy terms. A more balanced situation was found above the stable layer with the buoyancy term as a sink instead of a source. Hence, the imbalance or residual term I has been estimated to be ~15% of the largest term, as opposed to

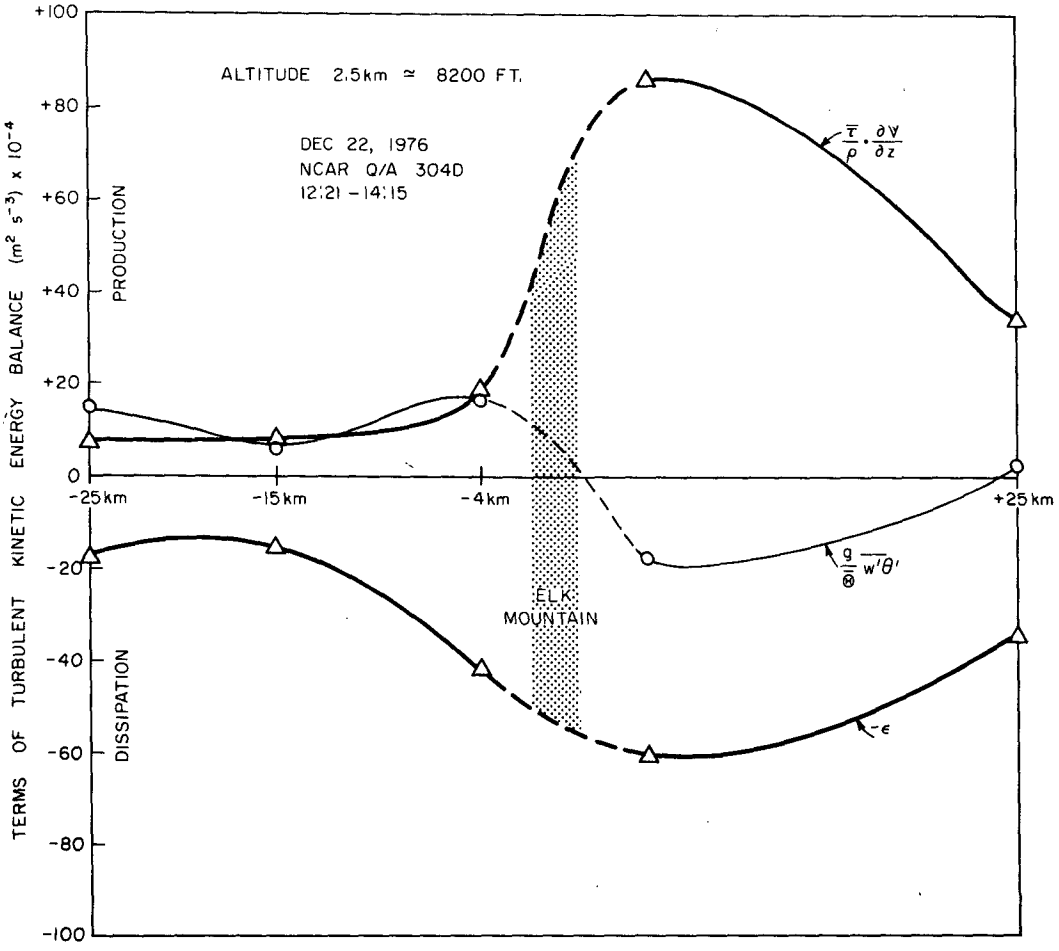

FIG. 11. Horizontal profile of TKE budget across ELK at 2.5 km MSL. Each plotted point represents an average for several different blocks over the entire flight leg.

~20% in the downwind area. The buoyancy term was a sink term in the downwind area. It is speculated that the cause of the imbalance term is due to the neglected terms, like the horizontal advection and pressure transport terms. Fig. 4c presents a vertical cross section of the mean turbulent kinetic energy [$\bar{e} = \frac{1}{2}(\overline{u'^2} + \overline{v'^2} + \overline{w'^2})$] upwind and downwind of ELK, demonstrating the possible importance of the horizontal advection term over mountainous terrain. Several other factors arise as possible contributors to the imbalance term. Inhomogeneity is felt to be the most important factor and should be considered over mountainous terrain, but stationarity and the statistical sampling errors may also contribute to the imbalance.

Acknowledgments. The authors gratefully acknowledge the assistance and recommendations of Drs. D. H. Lenschow and W. R. Lindberg.

The Elk Mountain data were collected under NSF Grant #DES(ATM) 75-02512. This research has also been sponsored by the Division of Atmospheric Water Resources Management, Bureau of Reclamation, U.S. Department of the Interior under Contracts 14-06-6801 and 7-07-83-V0001. The authors gratefully acknowledge the NCAR Research Aviation Facility for providing the aircraft, instrumentation and data recording system.

REFERENCES

Caughey, S. J., and J. W. Wyngaard, 1979: The turbulence kinetic energy budget in convective conditions. *Quart. J. Roy. Meteor. Soc.*, **105,** 231–239.

Champagne, F. H., C. A. Friehe, J. C. LaRue and J. C. Wyngaard, 1977: Flux measurements, flux estimation techniques, and fine-scale turbulence measurements in the unstable surface layer over land. *J. Atmos. Sci.*, **34,** 515–530.

Eaton, F. D., and R. A. Dirks, 1977: Turbulent flux measurements in the urban-rural atmosphere of greater St. Louis. *Preprints Sixth Conf. Inadvertent and Planned Weather Modification.* Campaign-Urbana, Amer. Meteor. Soc., 17–20.

Kaimal, J. C., J. C. Wyngaard, D. A. Haygen, O. R. Coté, Y. Izumi, S. J. Caughey and C. J. Readings, 1976: Turbulence structure in the convective boundary layer. *J. Atmos. Sci.*, **33,** 2152–2169.

Karacostas, T. S., 1978: Transport and turbulent diffusion over mountainous terrain. M.S. thesis, University of Wyoming, 116 pp.

LeMone, M. A., 1973: The structure and dynamics of horizontal roll vortices in the planetary boundary layer. *J. Atmos. Sci.*, **30,** 1077–1091.

Lenschow, D. H., 1970: Airplane measurements of planetary boundary layer structure. *J. Appl. Meteor.*, **9,** 874–884.

——, 1972: The measurement of air velocity and temperature using the NCAR Buffalo aircraft measuring system. NCAR Manuscript No. 71–219, 38 pp.

——, 1973: Two examples of planetary boundary layer modification over the Great Lakes. *J. Atmos. Sci.*, **30,** 568–581.

——, 1974: Model of the height variation of the turbulent kinetic energy budget in the unstable planetary boundary layer. *J. Atmos. Sci.*, **31,** 465–474.

Lumley, J. L., H. A. Panofsky, 1964: *The Structure of Atmospheric Turbulence.* Wiley, 289 pp.

Myrup, L. O., 1969: Turbulence spectra in stable and convective layers in the free atmosphere. *Tellus*, **21,** 341–354.

Mendenhall, W., and R. L. Schaeffer, 1973: *Mathematical Statistics with Applications.* Buxbury Press, 561 pp.

Pennell, W. T., and M. A. LeMone, 1974: An experimental study of turbulence structure in the fair-weather trade wind boundary layer. *J. Atmos. Sci.*, **31,** 1308–1323.

Vinnichenko, N. K., N. Z. Pinus, S. M. Shmeter and G. N. Shur, 1973: *Turbulence in the Free Atmosphere.* Central Aerological Observatory, Dolgoprudny, USSR. [Translated from Russian by John A. Dutton, Pennsylvania State University, for the Consultants Bureau, New York], 263 pp.

Wyngaard, J. C., and O. R. Coté, 1971: The budgets of turbulent kinetic energy and temperature variance in the atmospheric surface layer. *J. Atmos. Sci.*, **28,** 190–201.

Zubkovskiy, S. L., and B. M. Koprov, 1970: On the turbulent energy balance in the boundary layer of the atmosphere. *Izv. Atmos. Oceanic Phys.*, **6,** 589–592.